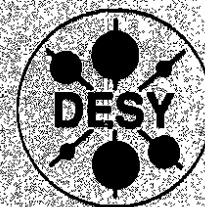


DEUTSCHES ELEKTRONEN – SYNCHROTRON



DESY 92-026
February 1992



**Hard Photoproduction
of Multiparticle Hadronic Final States**

E. Paul

Physikalisches Institut, Universität Bonn

ISSN 0418-9833

NOTKESTRASSE 85 · D - 2000 HAMBURG 52

DESY behält sich alle Rechte für den Fall der Schutzrechtserteilung und für die wirtschaftliche Verwertung der in diesem Bericht enthaltenen Informationen vor.

DESY reserves all rights for commercial use of information included in this report, especially in case of filing application for or grant of patents.

**To be sure that your preprints are promptly included in the
HIGH ENERGY PHYSICS INDEX,
send them to the following (if possible by air mail):**

DESY Bibliothek Notkestraße 85 W-2000 Hamburg 52 Germany	DESY-IfH Bibliothek Platanenallee 6 O-1615 Zeuthen Germany
---	---

1. Introduction

In this talk I review the experimental results available and those to be expected from hard photoproduction of multiparticle final states and discuss comparisons to QCD predictions.

The data include scattering processes with real photon beams and with almost real spacelike photons (of low Q^2) provided by muon and electron beams.

2. Phenomenology

The photon interacting with matter can be described as a superposition of a direct or pointlike component where the photon acts directly as the gauge boson of the electromagnetic field on the charges and the magnetic moments of the matter, and a hadronic component where the picture is that the photon is already in a hadronic state when entering into the strong interaction with matter: $\gamma = \text{direct } \gamma + \text{hadronic } \gamma$. The existence of initial hadronic photon states is permitted by the uncertainty principle. The simplest case when the hadronic state consists of a qq pair (fig. 1a) can be identified with the direct photon coupling. According to perturbative QCD theory there are corrections due to strong interactions (fig. 1b) which become large when the qq mass is small, and where at some stage bound states are formed (fig. 1c). It is of practical importance to subdivide the hadronic photon state into perturbative and non-perturbative part which border at some value of the mass of the hadronic system¹.

The perturbative component is called anomalous² or resolved³: The photon is a source of free quarks and gluons described by the hadronic structure functions of the photon for which calculations in QCD have been made possible by Witten's operator product expansion⁴.

The non-perturbative component is phenomenologically described by the Vector Meson Dominance (VMD) Model⁵ which assumes vector meson states are formed. The VMD component is responsible for the soft photoproduction processes (fig. 2) which account for most of the total photoproduction cross section.

Hard processes are related to direct, resolved and vector meson-like photon component. There are two QCD Born-term processes initialized by a direct coupling photon which are particularly simple and interesting in themselves: the so-called QCD-Compton process (fig. 3a) where the photon couples to a quark from the proton and a gluon is emitted, and the so-called γ -fusion process (fig. 3b) where the photon interacts with a gluon from the proton and a qq pair is created. - Besides these Born term processes and HO corrections to them it is predicted to have hard processes where the resolved photon is involved. An example of such a process is gg-fusion (fig. 3c) where proton and photon provide a gluon. - Finally there is a tail from the hadron-like photon component into the hard regime (fig. 3d) which may be estimated from scattering experiments with hadronic beams scaled by a VMD factor.

Most advanced are studies of the Born-term processes (figs. 3a and b). The QCD predictions (fig. 4) are of lowest order in α_s and depend on the usual Mandelstam variables as indicated. One has to define the QCD scale Q^2 for α_s and the proton structure functions. This definition is not straightforward, and for real and

Hard Photoproduction^{*} of Multiparticle Hadronic Final States

E. Paul^{**}

Physikalisches Institut der Universität Bonn
Nussallee 12, D-5300 Bonn 1, Germany

Abstract

Recent results from fixed-target experiments on the photoproduction of hadrons have shown that pointlike photon interaction processes of lowest order in QCD can be studied. These are the flavour-dependent γ -fusion process which is the key-process to explore the gluon structure function of the nucleon at small x_q and the QCD-Compton process which is a tool to study gluon fragmentation. The status of experimental results and comparison to QCD predictions is reviewed. The γ -fusion process will be measured in ep scatterings with almost real photons at HERA photon energies (equivalent to up to 50 TeV in the rest frame of the proton) down to $x_q \approx 10^{-4}$. Resolved (partonlike) photon interactions are predicted to be measurable at these high energies, too.

^{*}Invited talk at the XXI International Symposium on Multiparticle Dynamics, Wuhan, China, Sept 23 - 27, 1991

^{**}Supported by Bundesministerium für Forschung und Technologie, 05-5BN171/4, Bonn

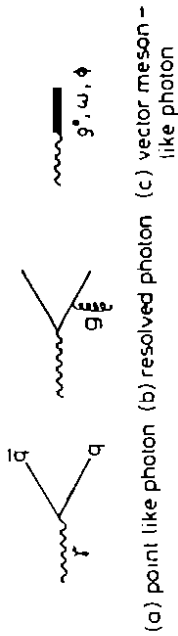


Fig. 1: Photon couplings

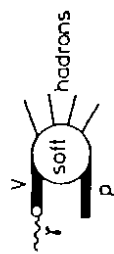


Fig. 2 Vector meson-like production of hadrons, $V = \rho^0, \omega, \phi, \dots$

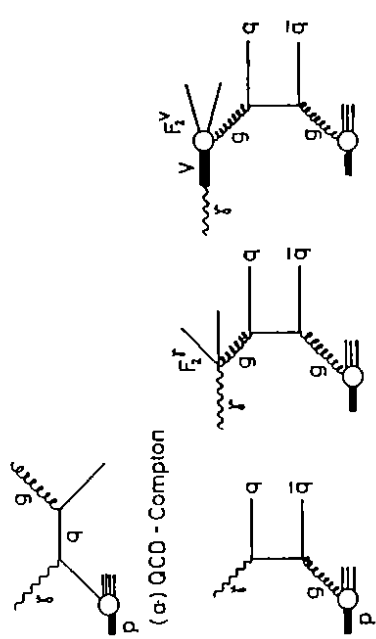


Fig. 3: Hard processes

$$\frac{d\sigma}{dt} = -\frac{4}{3} + 2\pi\alpha_s \alpha_e \frac{1}{s^2} \left(\frac{f}{s} + \frac{d}{s} \right)$$

$$\frac{d\sigma}{dt} = -\frac{1}{2} + 2\pi\alpha_s \alpha_e \frac{1}{s^2} \left(\frac{f}{s} + \frac{d}{s} \right)$$

QCD-Compton qg fusion

Fig. 4: QCD predictions for QCD-Compton and qg fusion

almost real spacelike photons examples of such definitions are:

$$Q^2 = -t \quad \text{squared 4-momentum transfer (from the photon to the initial gluon or quark)}$$

$$Q^2 = \frac{2sf\hat{u}}{s^2 + t^2 + \hat{u}^2} \quad \text{see Feynman}^6$$

$$Q^2 = -ap_T^2 \quad \text{squared transverse momentum of the final state parton}^2$$

$$Q^2 = \frac{m_{gq}^2}{2}, \frac{m_{qq}^2}{2} \quad \text{squared hadronic mass of QCD-Compton}^7, \gamma g\text{-fusion}$$

Quantitative QCD predictions depend, of course, on the definition of Q^2 which has been used, as does the comparison to data.

From the matrix elements of the Born-term graphs (fig. 4) the p_T slope can be estimated yielding $d\sigma/dp_T \propto p_T^{-4}$. On the other hand, the p_T slope of the VMD component can be expected to be as found from hadronic beams. For example in pp scattering at the ISR $d\sigma/dp_T \propto p_T^{-8}$ has been measured⁸, i. e. the p_T slope is much steeper than for the Born graphs with a cross over at a p_T -value of ~ 2 GeV (at fixed-target energies, fig. 5). This estimate is based on a QCD calculation² of the Born terms including HO corrections (which account for half of the cross section above $p_T > 2$ GeV, but affect p_T slopes etc. only slightly) and a VMD component calculated from measured cross sections with pion and kaon beams within the framework of the VMD model (see sect. 4). Existing data from fixed-target experiments cover a p_T -range up to about 5 GeV/c. This restriction to such relatively low

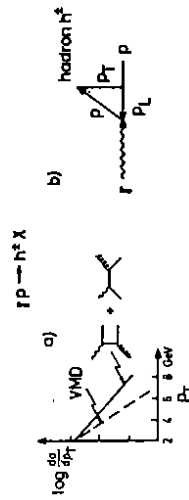


Fig. 5a: Predictions of VMD and pointlike component as a function of p_T of single charged particles;

Fig. 5b: Definition of p_T

p_T -values limits the possibilities to measure quantitatively QCD parameters at present.

The slope of the resolved photon processes lies inbetween the slope values of direct and VMD component discussed above. However, the cross section is small compared to the Born-term cross section at c.m.s. energies up to 30 GeV (an estimate is discussed in sect. 4).

table 1: Overview of the experiments; $q\bar{q}$ includes all quarks

generation	E_γ range	hard processes		
		experiments	direct γ	resolved γ
1	≤ 60 GeV	many; WA 57	low sensitivity	
2	60 - 400 GeV fixed target	NA14, NA14' WA69 E687 E691 E683 EMC : γ^* E665 : γ^* (low Q^2)	$q\bar{q}, c\bar{c}$ $q\bar{q}$ $q\bar{q}$ $c\bar{c}$ $c\bar{c}$ $q\bar{q}, c\bar{c}$ $q\bar{q}$	low sensitivity
3	≤ 50 TeV at the ep collider HERA	H1 : γ^* ZEUS : γ^* (low Q^2)	$q\bar{q}$ $c\bar{c}, b\bar{b}$	$q\bar{q}$ $c\bar{c}, b\bar{b}$

3. Photoproduction experiments

3.1. Overview

The experimental situation is summarized in table 1. A first generation of experiments with photon energies up to 60 GeV measured mainly soft photoproduction and total cross section.

A second generation of experiments is being carried out since the early eighties with photon and muon (virtual spacelike photon) beams of higher energies up to 400 GeV on fixed targets: NA14, WA69 at CERN and E687, E691, E683 at Fermilab with photon beams, and EMC at CERN and E665 at Fermilab with muon beams. Direct photon processes are studied either by the general onset at large p_T (together with some tail of the hadronlike component) or by measurement of charmed hadrons ($\gamma g \rightarrow c\bar{c}$) by means of active targets. Data was also taken with pion and kaon beams in the experiments NA14 and WA69 in order to estimate the VMD component.

The ep collider HERA will provide almost real photons (four-momentum transfer squared $Q^2 \approx 0$) of photon energies up to 50 TeV in the rest frame of the proton. The two forthcoming experiments H1 and ZEUS at this collider establish the third generation of experiments with precise measurements of direct photon processes, of light $q\bar{q}$ pairs, $c\bar{c}$ and $b\bar{b}$ separately. Moreover, the first experimental evidence of resolved photon processes can be expected.

In this talk I will review the main results from the fixed-target experiments which are underlined in table 1. Then I give a brief outlook in the near future at HERA.

3.2 Results from fixed-target experiments

The measurement of hard photoproduction began with the CERN-experiment NA14⁹. With photons of energies in the range from 50 to 150 GeV on a Be target the production of photon and hadrons at high p_T (> 1.6 GeV/c) was measured. One of the results proving the existence of the direct photon component is the inclusive cross section of π^0 production as a function of p_T .

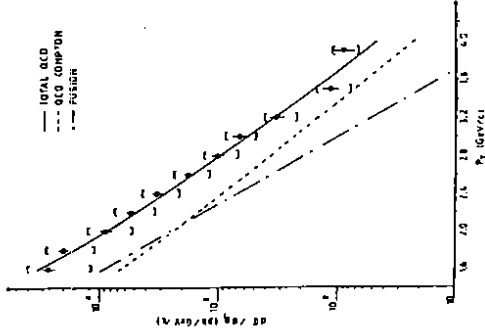


Fig. 6: Subtracted p_T distribution for inclusive π^0 photoproduction for $p_T > 40$ GeV (exp. Na 14). Statistical (vertical lines) and systematic errors are indicated.

In fig. 6 is shown the distribution obtained by subtracting from γ Be data π^0 data scaled by a factor of 1/200. The latter accounts for the vector meson-like photon component within the framework of the simple VMD model⁹. The distribution obtained (fig. 6) is compared to theoretical predictions²: a calculation of the two Born-terms (figs. 3a and b), and the total including Leading Log and next-to-LL terms. The predictions for γg -fusion and QCD-Compton shown separately indicate that the π^0 's with $p_T \geq 2$ GeV/c are primarily produced through the latter process.

Data and total prediction agree well in cross section and slope. The fit of the prediction has been carried out on this data imposing "known" structure functions of the proton and assuming for the gluon fragmentation function (QCD Compton) the ansatz:

$$D_f^\pi = (1-z)^{n_f} \quad \text{with } z = p'/p \text{ max.}$$

Two free parameters, besides Λ_{MS} the power n_f , were determined in the fit. The fit yielded¹⁰:

$$\Lambda_{MS} = 0.120_{-0.050}^{+0.105} \text{ and } n_f = 1_{-0.50}^{+0.55}$$

i. e. Λ_{MS} is consistent with other determinations, whereas $n_s = 1$ suggests that the gluon fragmentation is as hard as that of quarks. There are, of course, unknown systematic errors related to the uncertainties of the proton structure function and the subtraction method. However, the main result that the direct photon component is visible at large p_T is beyond any doubt.

The experiment WA69 was carried out at the multiparticle spectrometer OMEGA¹¹. In comparison to NA14 the photon energy range is slightly higher ($70 < E_\gamma < 170$ GeV) and a H_2 target was used instead of Be. Charged (and neutral) particle multiplicities were measured covering the whole range of soft and hard p_T . Data were taken with photon beam and with hadron beams (of π^\pm and K^\pm at 80 and 140 GeV/c) in the same apparatus. The hadron beams were needed to estimate the VMD component by combining πp and $K p$ cross sections in the ratio 2 : 1 in order to represent the quark content of the light vector mesons ρ^0 , ω and ϕ , and applying an appropriate VMD factor which accounts for the relative coupling strength of the vector mesons to the photon.

The inclusive production of charged particles measured by WA69 in the whole p_T range (from 0 to 5 GeV/c) is shown in fig. 7a. The γp data fall less steep than the VMD component; the ratio of cross sections demonstrates more clearly the onset of the direct component in the γp data at high p_T (fig. 7b). The appropriate VMD factor which implies a ratio of 1 at low p_T was found to be 1/215. This value is consistent with other measurements (via σ_{tot} and elastic vector meson production) and with simple quark model predictions¹². The VMD factor has been determined in experiment WA69 also from inclusive ρ^0 production¹². Restricting the kinematical range of the ρ^0 to $x_F < 0.7$ and $p_T < 1.6$ GeV the value of the VMD factor was determined to be $1/(205.8 \pm 3.5)$. The distribution obtained by subtraction of the two distributions in fig. 7a from each other is shown in fig. 7c in comparison to QCD predictions: the one from Aurenche et al.², discussed already in context with NA14, is given by full and dashed line (with and without anomalous component), and a prediction obtained with the program LUCIFER¹³, accounting only for the Born-term graphs (fig. 4) and fragmenting the outgoing partons to hadrons in the LUND scheme by means of JETSET¹⁴. Both types of predictions, i. e. with and without HO corrections describe the gross features of the data (absolute cross section, p_T slope) correctly suggesting that the influence of HO-corrections is small.

In WA69 the Born term processes were also studied in terms of angular energy flows¹⁷ based on the measured charged particle final states. LUCIFER predicts a dip in forward direction (i. e. at small angles w.r.t. the photon beam) according to the back-to-back property of the two Born-term partons in the final state. The problem is that the cut in $\Sigma p_{T,vis}^2$ (where $p_{T,vis}$ is the p_T of a charged particle in the final state in the event plane), which is applied to remove soft processes also causes a dip due to phase space restriction. Comparing γp data with the scaled hadron beam data (VMD component) a dip growing with $\Sigma p_{T,vis}^2$ is visible in both data sets, however more pronounced in the γp data (fig. 8). The difference distribution (fig. 9) is well described by the LUCIFER prediction of the Born-terms (histogram). The energy sharing of the two back-to-back partons is another feature of the Born-term processes to be tested. It can be made visible by ordering the energy clusters for each event so that the smaller one is drawn in at negative angle whereas the larger one is at positive angle. Data and prediction from LUCIFER agree well also with respect to this feature (fig. 10).

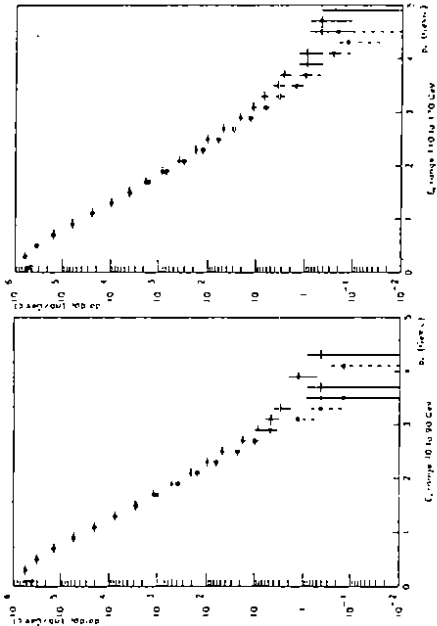


Fig. 7a: Single inclusive cross sections of charge hadrons as a function of p_T ; full circles: photon-beam data, open circles: normalized hadron-beam data (exp. WA 69)

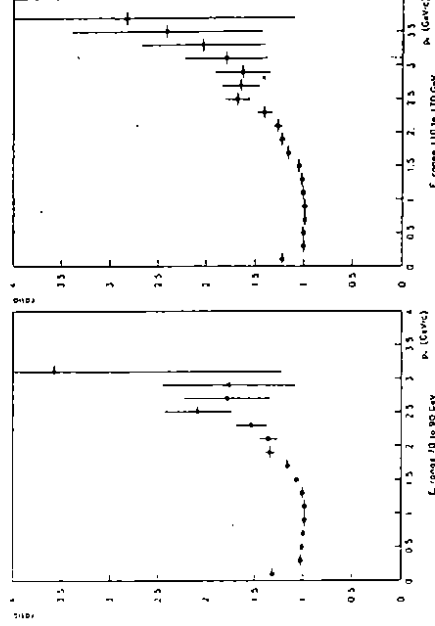


Fig. 7b: Ratio of photon-beam data to normalized hadron-beam data as a function of p_T integrated over $0 < x_F < 0.7$ (exp. WA 69)

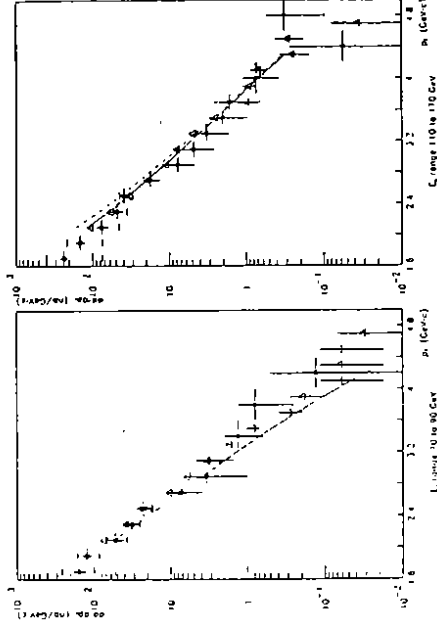


Fig. 7c: Subtracted p_T distributions integrated over $0 < x_F < 0.7$; full circles: data points (exp. WA 69), full and dashed lines: predictions by Aurenche et al. (see text); triangles: predictions by LUCIFER (see text)

Fig. 8: Energy flow distributions for bins of Σp_{T0}^2 as indicated; full triangles: photon-beam data; open triangles: normalized hadron-beam data (exp. WA 69)

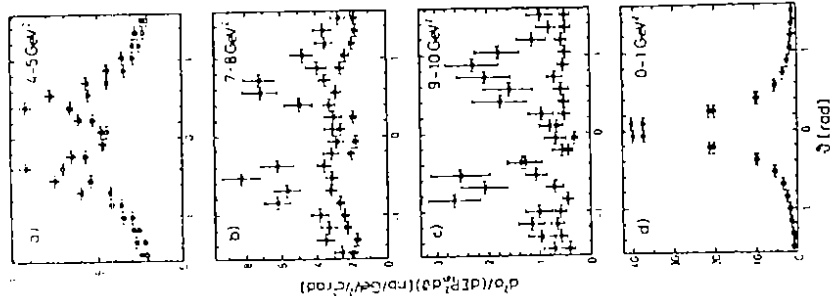


Fig. 10: Subtracted asymmetric energy flow data (exp. WA 69)

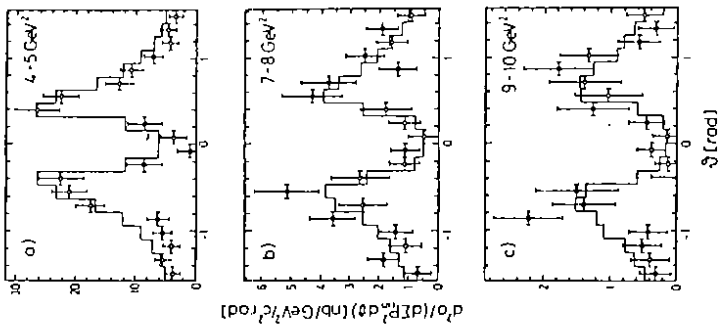
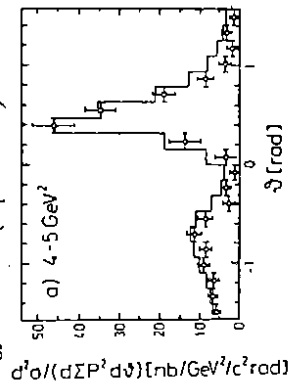


Fig. 9: Subtracted energy flow data corresponding to fig. 8 in comparison to LUCIFER (histogram)

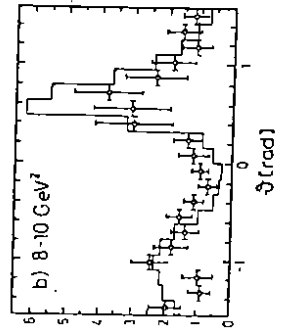


Fig. 11: Higher-Twist

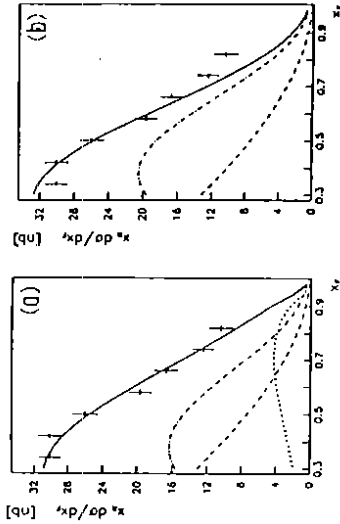
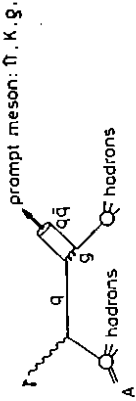


Fig. 12a: Fitted x_F distribution of charged particles of $p_T > 2$ GeV/c (γp data, $110 < E_\gamma < 200$ GeV, exp. WA 69); full line: Born-terms; dashed: hadron-like photon component, dotted: Higher-Twist component

Fig. 12b: Corresponding fit with a Higher-Twist component fixed to zero

Next we consider the inclusive x_F distribution of charged hadrons from experiment WA69. It has been proposed to look there for contributions from Higher Twist¹⁵ (HT) of the type indicated in fig. 11. The x_F distribution of the γp data restricted to $p_T > 2$ GeV/c (fig. 12) was fitted to a linear superposition of three cross sections¹⁶: VMD component (calculated from γp and $K p$ measurements, scaled by the VMD factor), Born-terms (from LUCIFER) and HT, also predicted by LUCIFER. The fit finds a significant HT signal (fig. 12a) with a cross section of the order of magnitude predicted¹⁵. When fixing the HT component to zero the data are not well fitted by the other two components alone (fig. 12 b).

In the Fermilab experiment E691 the photoproduction of charmed mesons on Be was measured¹⁸ and the analysis was based on a comparison to a prediction for the γg -fusion process ($\gamma g \rightarrow c\bar{c}$) where next to leading order corrections were included¹⁹. Diffraction-like photoproduction of charm was excluded by kinematical cuts. The charm photoproduction cross section is sensitive to the uncertainty of the mass of the charm quark, since over the entire energy range studied ($80 < E_\gamma < 230$ GeV) threshold effects are still present. A fit to the data was carried out including x_F and p_T distributions of inclusive D (fig. 13) and $\sigma_{tot}(c\bar{c})$ in order to determine simultaneously m_c and n_g , a parameter defined via

$$G(x_g) = (1 - x_g)^{n_g}$$

for the gluon distribution of the proton. The fit yielded:

$$m_c = 1.74^{+0.13}_{-0.18} \text{ GeV and } n_g = 7.1 \pm 2.2$$

A similar study is in progress in Fermilab experiment E687²⁰ which was carried out at the highest energies so far ($100 < E_\gamma < 400$ GeV). Measurements of inclusive D, D' production and σ_{tot} ($c\bar{c}$) were analysed in terms of γg -fusion¹⁹. The total charm cross section (fig. 14) shows the comparison to the predictions assuming $m_c = 1.5$ GeV, the QCD scale parameter $\Lambda = 260$ MeV and $Q^2 = 10$ GeV² (full line) and for Λ changed by ± 100 MeV and Q^2 changed by a factor of 2 (dashed lines). It has been pointed out that there are strong correlations between the parameters to be set (m_c , Λ , Q^2 , gluon structure function) which cannot be resolved in the "low p_T range" measured at these (low) energies, but again, as for E 687, the default choices of the parameters lead to satisfactory descriptions.

Finally I consider briefly preliminary results from Fermilab experiment E665 where forward di-jet production was observed in μp and μd interactions²¹. Distributions of p_T of hadronic jets (i. e. $\Sigma p_{T, \text{had}}$) and angular energy flows were studied in the range $20 < E_\gamma < 500$ GeV and $100 < W^2 < 500$ GeV² (where W is the mass of the hadronic system). The authors claim that the angular flow distributions are as expected from perturbative QCD.

3.3 Photoproduction in ep collisions at HERA

In the near future photoproduction experiments are carried out with spacelike almost real photons at very high energies. At HERA the two experiments H1 and ZEUS are going to measure interactions of 30 GeV electrons with 820 GeV protons, which provide a c.m.s. energy of 314 GeV and energies of the spacelike photon up to 52 TeV in the rest frame of the proton. This extends the range of p_T covered in fixed-target experiments by an order of magnitude. At large transverse momenta the direct photon Born-term processes dominate over the DIS processes which are suppressed by a factor of $1/Q^2$. The QCD-Compton process (fig. 15a) is predicted⁷ to be measured at HERA energies up to a p_T value of at least 40 GeV/c (fig. 16).

The γg -fusion process (fig. 15b) allows the measurement of the gluon distribution of the proton. The latter is at present poorly determined at small x ($x < 0.1$); on the other hand, theoretical predictions are most interesting at small x as it was discussed for instance by Close at the Singapore conference²². A measurement in this range could clarify how to extrapolate QCD into the semi-hard region. At HERA energies the structure functions can be measured down to x -values of $\sim 10^{-4}$ and so also x_g (x of the gluon) which is related to x by:

$$x_g = x \left(1 + \frac{m_c^2}{Q^2} \right) \quad \text{where } Q^2 \text{ is the squared 4-momentum of the virtual photon.}$$

The γg -fusion process can be isolated from most of the other processes by measuring the two-jet production of $c\bar{c}$ and $b\bar{b}$ for which the cross sections are large. The final calculation of x_g of the proton from those measurements requires theoretical input as well since gluon bremsstrahlung off the initial gluon and other HO corrections are not small²³. The gluon distribution of the proton will be further studied at HERA by measuring J/ψ production (fig. 15c) and moreover via the longitudinal structure function F_L (where at small x the dominant contribution comes from the gluon distribution).

Fig. 13: $\gamma \text{Be} \rightarrow D^*, D^+ X$ (exp. E 691): x_F dependence (a) and p_T^2 dependence (b) of D production

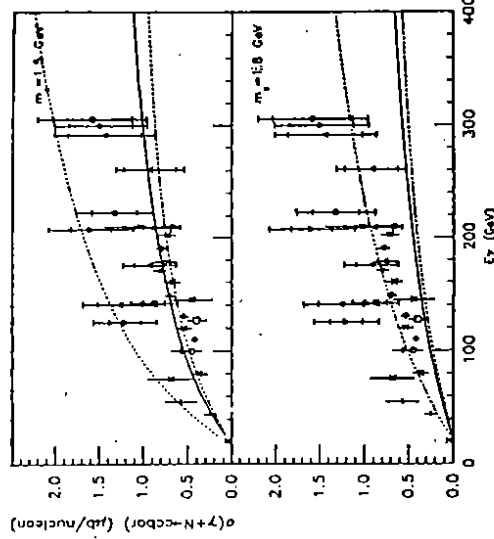
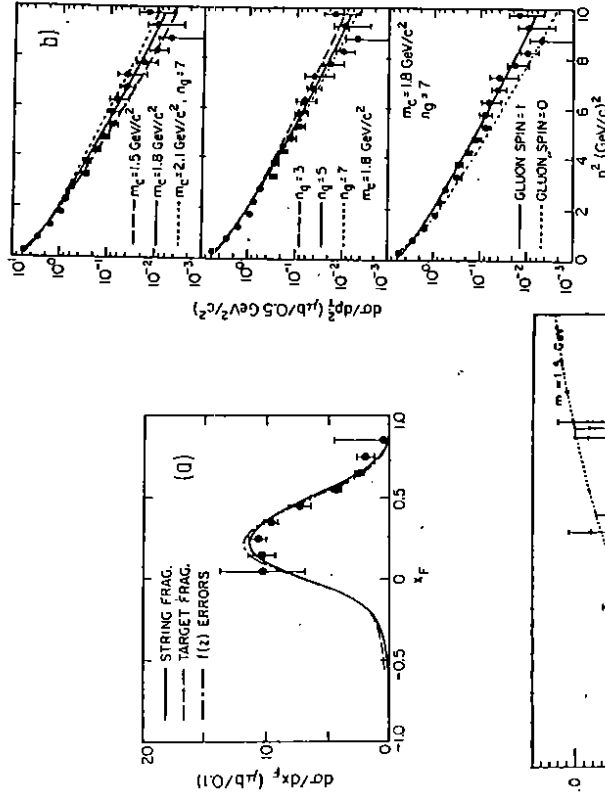


Fig. 14: Total cross section per nucleon for photoproduction of open charm events vs. photon energy in comparison to QCD predictions constrained by m_c and the QCD-parameter Λ (exp. E 687); solid curve: $\Lambda = 260$ MeV, $Q^2 = 10$ GeV²; dashed curve: Λ changed by ± 100 MeV and $Q^2 = 20$ GeV².

The present knowledge about the gluon structure function of the photon is poor. A first estimate has been achieved from $\gamma\gamma$ data by means of a phenomenological evolution²⁵ (fig. 18). New data from TRISTAN and LEP will be very helpful.

There is a wide variety of parton processes with quarks and gluons from both proton and photon, see e. g. fig. 19. A recent calculation³ of the individual cross sections and their sum which depend on the structure functions assumed is shown in fig. 20. They are large in comparison to the direct photon component at moderate P_T of about 10 GeV/c (fig. 21) where the HERA experiments are well suited to measure them.

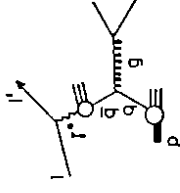


Fig. 19:
Parton process with quark from the proton and anti-quark from the virtual resolved photon

The total photoproduction cross section is expected to increase with c.m.s. energy²⁶. Considering parton processes, such a rise can be caused by γg and $g g$ fusion processes whose cross sections grow with increasing energy since the x_g range is extended to lower x_g values covering the so-called semihard region, i. e.

$$\sigma_{tot} = \sigma_{soft} + \sigma_{semihard}(S).$$

A measurement of σ_{tot} is planned at HERA. It will provide an interesting global check of the parton processes assumed and structure functions introduced in order to analyse photoproduction.

I would like to thank my colleagues B. Diekmann and K. Heinloth and J. Crittenden for careful reading of the manuscript.

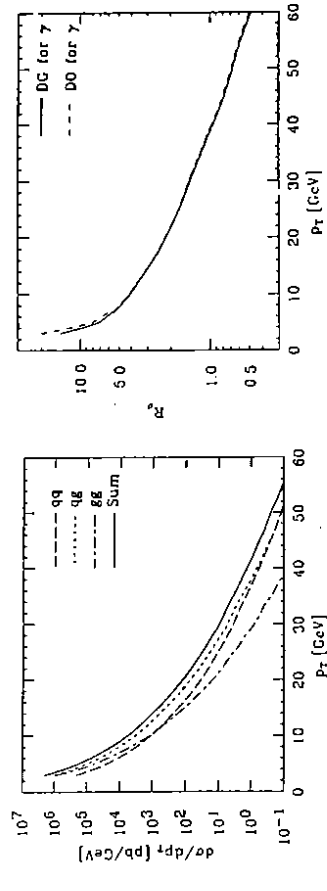


Fig. 20: Predicted cross sections for parton processes with resolved photon yielding 2-jets in the final state
Fig. 21: Predicted ratio of resolved-photon to direct contributions for two-jet production at HERA for two sets of structure functions

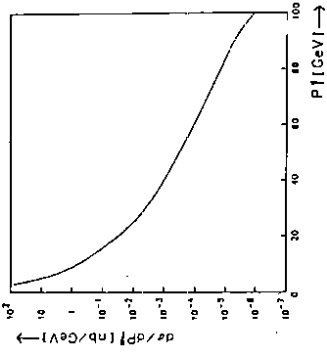
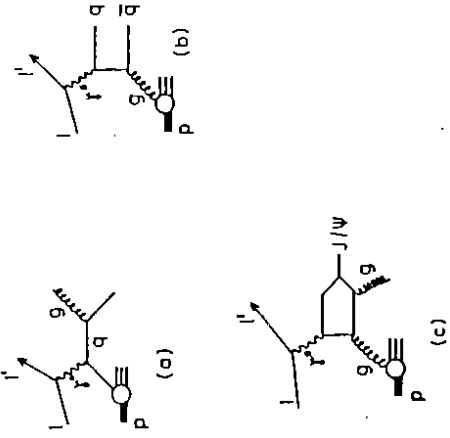


Fig. 16:
QCD-Compton or gluon bremsstrahlung (a), γg fusion (b) and J/ψ production (c) in ep scatterings
Fig. 17: Valence part (A) and sea part (B) of Witten's leading log calculation



At HERA energies photoproduction also probes the photon structure function F_2^γ which has been calculated first by Witten. His result²⁴ (fig. 17) shows the characteristic feature (at large Q^2): a valence quark distribution which peaks at relatively large x and a sea quark distribution peaking at low x as usual.

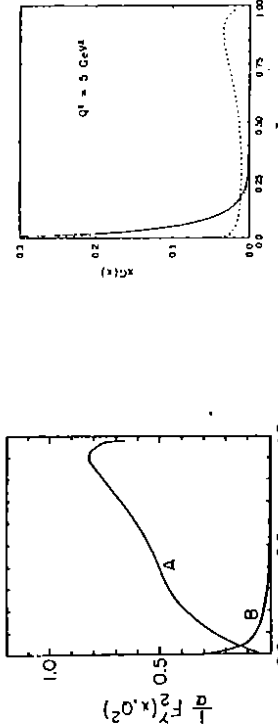


Fig. 17:
Valence part (A) and sea part (B) of Witten's leading log calculation
Fig. 18:
Gluon distribution of the (resolved) photon determined from data for different parametrizations

4. References

1. see e.g. M. Glück and E. Reya, *Phys.Rev. D28* (1983) 2749
2. P. Aurenche et al., *Nucl.Phys. B286* (1987) 553
3. M. Drees and R.P. Godbole, *Phys.Rev.Lett. 61* (1988) 682
4. E. Witten, *Nucl.Phys. B120* (1977) 189
5. see e.g. T.H. Bauer et al., *Rev.Mod.Phys. 50* (1978), 261;
E. Paul, *Lecture Notes in Physics*, Vol. 365 p. 55, Springer Verlag 1990
6. R.P. Feynman, R.D. Field and G.C. Fox, *Phys.Rev. D18* (1978), 3320
7. J.J. Engelen et al., *NIKHEF-H*, 189-3
8. W.M. Geist et al., *Phys.Rep. 197* (1990) 263
9. E. Auge et al., *Phys.Lett. 168B* (1986) 163
10. D. Treille, *Workshop on QCD in St. Croix, 1987, NATO ASI Series B: Physics Vol. 197*, p. 193;
G. Wormser, *Lecture Notes in Physics*, Vol. 365 p. 100, Springer Verlag 1990
11. R.J. Apsimon et al., *Z.Phys. C43* (1989) 63
12. R.J. Apsimon et al., to be published in *Z.Phys. C*
13. G. Ingelmann and A.S. Weigend, *DESY-87-018*
14. B. Anderson et al., *Phys.Rep. 97* (1983) 31
15. M. Benayoun, *Nucl.Phys. (Proc.Suppl.) 7B* (1989) 205
16. R.J. Apsimon et al., *Z.Phys. C50* (1991) 179
17. R.J. Apsimon et al., *Z.Phys. C46* (1990) 35
18. J.C. Anjos et al., *Phys.Rev.Lett. 65* (1990) 2503
19. R.K. Ellis and P. Nason, *Nucl.Phys. B312* (1989) 551
20. E687 Collaboration, *FERMILAB-CONF. 90/261-E*, paper submitted to the XXV. Int.Conf. on HE Physics, Singapore 1990
21. E665 Collaboration, paper submitted to the XXV. Int.Conf. on HE Physics, Singapore 1990
22. F. Close, *Proc. of the 25th. Int. Conf. on HE Phys.*, Vol.1 p. 213, Singapore 1990
23. G. Schuler, *Proc. of HERA Physics Workshop 1991*, to be published
24. D.W. Duke, *Proc. of the 5th Workshop on Photon-Photon Collisions*, p. 251, Aachen, 1983
25. H. Abramowicz, U. Charcula, A. Levy, *DESY 91-069*
26. A. Levy, *Proc. of the HERA Physics Workshop 1991*, to be published